Transport and Dynamics of Nonequilibrium Phonons in Single-Crystal Ruby Fibers

S. A. Basun, S. P. Feofilov, and A. A. Kaplyanskii
A. F. Ioffe Physical-Technical Institute, 194021 St. Petersburg, U.S.S.R.

W. M. Yen
Department of Physics and Astronomy, University of Georgia, Athens, Georgia 30602
(Received 12 August 1991)

The transport of 29-cm^{-1} phonons in single-crystal fibers of Al_2O_3:Cr^{3+} (ruby) has been investigated at 2 K. The fiber diameters are of the order of the mean free path, so that transport is dominated by diffuse scattering and by acoustic mismatch at the lateral crystal interfaces. Depending on experimental conditions, we have observed ballistic and diffusive phonon transport. We determine for the first time the probability of frequency nonconserving surface scattering for high-frequency phonons.

PACS numbers: 63.20.Hp, 63.20.Mt, 78.50.Ec

Phonon-interface interactions are central to energy transport across boundaries. A number of studies have addressed their interaction with high-quality crystal surfaces. Strong specular reflection of GHz phonons from an Al_2O_3 surface has been reported [1] and it has been shown that diffuse scattering increases with increased phonon energies [2]. In this Letter, we describe the behavior of phonons in thin, single-crystal fibers of ruby which have become available recently. The geometry is particularly attractive because it accentuates scattering at the surfaces. The fiber diameters can be chosen to be comparable to the mean free path $\bar{l}$ of high-frequency (THz) phonons at low temperatures. Our studies corroborate results obtained at lower phonon frequencies; in addition, we have determined for the first time the relative probabilities of frequency conserving versus nonconserving phonon scattering at our fiber surfaces.

Single-crystal fibers of 0.02 at.% ruby ($D=400$ μm, $L=2$ cm) oriented with the c axis either parallel or perpendicular to the fiber axis were grown using the laser heated pedestal growth (LHPG) method [3]. Prior studies (R-line widths and break point) indicate that the fibers are of very high crystalline quality; defects and imperfections are expected to be mostly in the surface region [4].

Experiments were performed using injected broad-band and narrow-band nonequilibrium phonons. 29-cm^{-1} phonons were detected using the R_2 luminescence of Cr induced by their passage through a volume excited by an Ar laser beam (514 nm) [5], labeled d in Fig. 1. For broad-band injection, a 10-nm-thick, 0.3-mm^2 Constantan heater film (10 Ω) was evaporated on the fiber surface near one end of the fiber, labeled h in Fig. 1. With current pulses of 200 ns, energy densities of 0.1–10 μJ/mm^2 could be generated.

A pulsed ($\Delta t=20$ ns) Cu-vapor laser (510- and 578-nm lines), operating at 10 kHz and average power ranging from 30 mW to 1.5 W, was used to excite the $^4T_2$ absorption of ruby. In this case, the phonon spectrum generated contains a sharp peak at 29 cm^{-1}, resulting from intralevel relaxation within the ^2E states [6]. With the use of a cylindrical lens, 10 mm of the fiber could be illuminated; phonons are detected in the middle of the excited volume [see Fig. 3(b) inset]. Since the interval between pulses is shorter than the R_1 lifetime ($\tau_R \simeq 4$ ms), the irradiation creates a quasistationary excited Cr^{3+} population, N_E, in the sample volume from which phonons can be trapped or scattered.

Experiments were performed with the fiber either totally or partially immersed in He II (2 K) [see Fig. 1 (levels A and B)]. In the latter case, the experimental area is surrounded with He gas at 20 Torr. The degree of immersion provides a means to vary the acoustic mismatch encountered by phonons at the fiber surface.

The propagation of 29-cm^{-1} phonons was studied for both c-axis orientations as a function of $x=h-d$, input power, and degree of fiber immersion. With broad-band

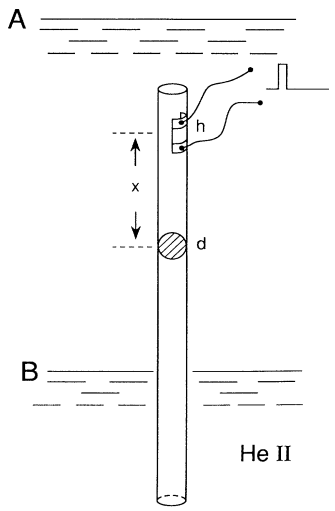

FIG. 1. Diagram of heat-pulse experiments on the single-crystal ruby fibers. Heater is labeled h, detection region by d, and $x=h-d$; A and B denote the He II levels employed in the experiments.

injection and with the sample fully immersed, $R_2(t)$ is shown as a function of x in Fig. 2(a). The phonons detected result directly from injection or are by-products of scattering processes from other modes of the quasicontinuum. The onset of the signal maintains its rise time (<1 μs) throughout, while the signal broadens modestly in time as x increases. Further, the signal magnitude is found to decrease as x^{-3} consistent with ballistic propagation from an off-axis small planar source. The character of $R_2(t)$ changes dramatically when the experimental region is surrounded by He gas [see Fig. 2(b)]. The leading edge loses it sharpness with the rise time slowing as x increases and the wave form broadens. A persistent signal also begins appearing at very long times, e.g., signals last up to $t_e=30$ μs.

The changes observed in $R_2(t)$ as a function of immersion and x (Fig. 2) may be understood qualitatively in terms of the interaction of the phonons with the fiber surface, where they can undergo specular or diffuse reflections with random angles. Diffusely scattered phonons can readily escape the fiber if the surfaces are in contact with He II through the so-called "helium effect" (anomalous Kapitza transmission [7]). In Fig. 2(a), the signal is consistent with the exclusive detection of nearly axially propagating ballistic 29-cm^{-1} phonons, which have undergone either none or a small number of grazing specular reflections. For multiple reflections, phonons have a near-unity probability of escape into the liquid as the mean surface reflectivity has been estimated to be $\sim$80% [8]. In other words, the fiber acts as a spatial filter for axial, ballistic phonons.

The pulse shape at $x=0$ is found to be dependent on the heater power. At low powers (0.1 μJ/mm^2), the

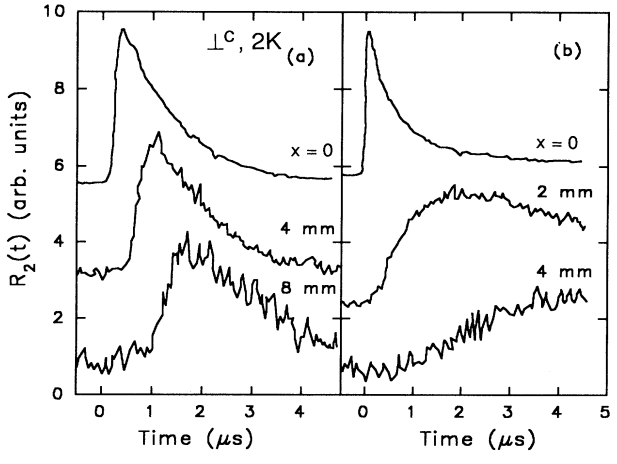

FIG. 2. 29-cm^{-1} phonon-induced fluorescence-detection signals, $R_2(t)$, in heat pulse experiments shown as a function of x: (a) fiber fully immersed in He II, and (b) fiber partially immersed with experimental region in contact with He gas. Traces are for the c axis perpendicular to fiber axis; $T=2$ K. Heater power at 10 μJ/mm^2.

$R_2(t)$ replicates the heater pulse; as power is increased, the signals broadened, reaching a width of 1.5 μs at 10 μJ/mm^2 (Fig. 2). This dependence is characteristic of a "hot spot" in the heater region and is indicative of strong phonon scattering [9]; given the excellent bulk quality of the fiber samples [4], and the fact that hot spots are generally not observed in dilute ruby, their existence here lends support to our assertion that phonon interactions occur near the fiber walls.

The leading edge of $R_2(t)$ shown in Fig. 2(a) for the $\perp c$ fiber is characteristic of ballistic transport. The arrival time of the edge is linearly proportional to x, yielding a velocity of $v_l=11$ km/s, appropriate for LA sound velocities in ruby [10]. In the case of the $\|c$ fiber, $R_2(t)$ behaves in a similar fashion but the pulses are narrower and the leading edge is slower in arriving at d (not shown). Here, LA phonons cannot contribute to the $R_2(t)$ luminescence [11], allowing us to conclude that $v_l=6$ km/s, corresponding to the TA sound velocity. Pulse broadening as a function of x occurs in both samples because of the delays incurred by phonons in undergoing a few reflections; broadening is more severe in the $\perp c$ sample since in this case both the LA and the slower TA phonons have a distribution of arrival times and therefore cannot be separated temporally.

In case B, the phonons must travel to the immersed section of the fiber in order to escape. Their transport becomes diffusive as the result of multiple scatterings at the surfaces while propagating ballistically between events. The changes in the leading edge of $R_2(t)$, Fig. 2(b), reflect the effects of random nonspecular reflections. The situation is similar to Knudsen flow of a low-pressure gas in a tube [12], which is diffusive in one dimension. The peak arrival time of the phonon pulses at x is then given by

$$t=\langle x^2\rangle/\bar{l}v\,, \tag{1}$$

with v the flow velocity. Figure 2(b) yields $\bar{l}=0.5$ mm $\cong D$, as expected. Similarly, the propagation time before phonons reach the He II can be written as

$$t_e=L^2/Dv\,. \tag{2}$$

In our experiments, $L=10$ mm above He II, so that $t_e=40$ μs, in general agreement with the observations of a persistent $R_2(t)$ tail.

For narrow-band injection, results are shown in Fig. 3; phonons are detected at d (see the inset to Fig. 3). The decay of the original phonon population is monitored in these experiments. With the He II level at A, $R_2(t)$ replicates the heat-pulse results for all laser powers, while for level B, $R_2(t)$ retains a sharp leading edge in contrast to Fig. 2(b). A persistent tail begins to appear at higher pump powers. With monoenergetic generation, the sharp $R_2(t)$ pulses seen in Fig. 3 with the fiber fully immersed are a direct measure of the spatial escape of 29-cm^{-1} phonons from the excitation volume. At low powers

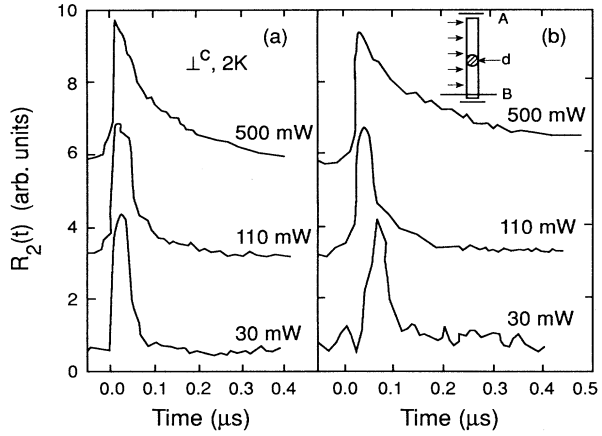

FIG. 3. $R_2(t)$ with monoenergetic phonon generation in a 10-mm section of fiber as a function of laser power: (a) fiber fully immersed in He II, and (b) excited volume over the superfluid level. Sample and temperature are as in Fig. 2. Inset: The experimental configuration with d denoting the detector; A and B are the He II levels.

($P=30$ mW, $N_E=10^{14}/\text{cm}^3$), the value of N_E leads to a mean free path for resonant scattering of 29-cm^{-1} phonons from the ^2E Cr levels of $\bar{l}_r=1$ mm, comparable to D [13]. Phonons escape in $t_1=150$ ns given by the $R_2(t)$ width; t_1 is slightly larger than the phonon ballistic time across D (50 ns). This is a situation which has been termed "marginal trapping" [14]. In such cases,

$$t_1=\frac{D}{v}\frac{1}{1-p}, \tag{3}$$

with p the phonon survival probability, i.e., the surface reflectivity in our case. Equation (3) yields $p=0.6$ and the probability of decay or escape is sizable, i.e., $1-p=0.4$.

The $R_2(t)$ shape in partial immersion and low laser powers, Fig. 3(b), is nearly identical to that observed for total immersion. Since phonons have no means to escape directly into the He gas, this leads to the important conclusion that the narrow-band 29-cm^{-1} distribution decays first by leaving the frequency mode in the scattering events and that these processes are independent of the surface contact. The similarities of the signals lead to parameters (l_r and t_1) which again satisfy the conditions of marginal trapping, this time in the frequency domain; p in Eq. (3) now becomes the probability of scattering with frequency conservation. It follows that frequency conserving versus nonconserving events occur with nearly equal probabilities, i.e., in a ratio of 6:4. This also allows us to conclude that, in general, inelastic scattering at the fiber surfaces precedes escape of the phonons from the excitation region into the He II when contact exists.

As N_E is increased, the $R_2(t)$ signals are consistent with "diffusion trapping" dominated by resonant elastic scattering from the excited Cr ions [14]. In such cases $\bar{l}\ll D$ and fiber surfaces and geometry play a minor role in the phonon dynamics. The origin of the long $R_2(t)$ tail observed in Fig. 3(a) at high laser powers is similar to that discussed earlier, indicating slow one-dimensional diffusion. As N_E reaches $10^{16\text{-}17}/\text{cm}^3$, strong resonant trapping of phonons occurs and the fiber geometry becomes irrelevant to the phonon dynamics [14].

We have shown that the availability and the geometry of single-crystal fibers provide us with new opportunities in the study of nonequilibrium phonons and their interactions with surfaces. We also conclude that high-frequency phonon reflection at interfaces is mainly diffuse and depends on the nature of the fiber-surface contact. As a result, the reflection processes can be elastic or inelastic with nearly equal probabilities.

The authors are grateful to Dr. V. L. Shekhtman, Professor R. S. Meltzer, and Professor W. M. Dennis for useful comments and discussions. Dr. B. M. Tissue and Dr. L. Lu of UGA provided the fibers. Work at Georgia was supported by NSF under Grant No. DMR 87-17696 and the collaboration by the U.S.S.R. Academy of Sciences and by the UGA Research Foundation.

[1] P. Taborek and D. L. Goodstein, Phys. Rev. B **22**, 1550 (1980).
[2] W. Eisenmenger, in *Phonon Scattering in Condensed Matter: V*, edited by A. C. Anderson and J. P. Wolfe (Springer-Verlag, Berlin, 1984), p. 204.
[3] B. M. Tissue, Lizhu Lu, and W. M. Yen, J. Lumin. **45**, 20 (1990).
[4] W. M. Yen, Proc. SPIE Int. Soc. Opt. Eng. **1033**, 183 (1988).
[5] K. F. Renk and J. Diesenhofer, Phys. Rev. Lett. **26**, 764 (1971).
[6] R. S. Meltzer and J. E. Rives, Phys. Rev. Lett. **38**, 421 (1977).
[7] H. Kinder, J. Weber, and W. Dietsche, in *Phonon Scattering in Condensed Matter*, edited by H. J. Maris (Plenum, New York, 1980), p. 173.
[8] A. A. Kaplyanskii, S. A. Basun, and V. L. Shekhtman, J. Phys. (Paris), Colloq. **42**, C6-439 (1981).
[9] H. M. Greenstein, M. A. Tamor, and J. P. Wolfe, Phys. Rev. B **26**, 5604 (1982); also K. Z. Troost, M. J. van Dort, J. I. Dijkhuis, and W. W. de Wijn, Phys. Rev. B **43**, 98 (1991).
[10] R. J. von Gutfeld and A. H. Nethercot, Phys. Rev. Lett. **17**, 1469 (1966).
[11] A. A. Kaplyanskii, S. A. Basun, V. A. Rachin, and R. A. Titov, Pis'ma Zh. Eksp. Teor. Fiz. **21**, 438 (1975) [Sov. Phys. Solid State **17**, 280 (1976)].
[12] See, e.g., C. Kittel and H. Kroemer, *Thermal Physics*, (Freeman, San Francisco, 1980), 2nd ed., p. 397.
[13] R. S. Meltzer, J. E. Rives, and W. C. Egbert, Phys. Rev. B **25**, 3026 (1982).
[14] A. A. Kaplyanskii and S. A. Basun, in *Nonequilibrium Phonons in Nonmetallic Crystals*, edited by W. Eisenmenger and A. A. Kaplyanskii (North-Holland, Amsterdam, 1986), p. 373.